LAWRENCE
LIVERMORE
NATIONAL
LABORATORY

LLNL-JRNL-446591

Demonstration of ignition radiation temperatures in indirect-drive inertial confinement fusion hohlraums

S. H. Glenzer, B. J. MacGowan, N. B. Meezan

August 2, 2010

Physical Review Letters

Disclaimer

Demonstration of ignition radiation temperatures in indirect-drive inertial confinement fusion hohlraums

S. H. Glenzer,[1] B. J. MacGowan,[1] N. B. Meezan,[1] P. Adams,[1] J. Alfonso,[1] E. Alger,[1] Z. Alherz,[1] L. Alvarez,[1] S. S.Alvarez,[1] P. Amick,[1] K. Andersson,[1] S. Andrews,[1] G. Antonini,[1] P. Arnold,[1] D. Atkinson,[1] L. Auyang,[1] S. Azevedo,[1] B. Balaoing,[1] J. Baltz,[1] F. Barbosa,[1] B. Bardsley,[1] D. Barker,[1] J. Baron,[1] R. Beeler,[1] B. Beeman,[1] L. Belk,[1] P. Bell,[1] R. L. Berger,[1] M. Bergonia,[1] L. Bernardez,[1] L. Bertolini,[1] R. Bettenhausen,[1] L. Bezerides,[1] S. Bhandarkar,[1] C. Bishop,[1] E. Bond,[1] D. Bopp,[1] J. Borgman,[1] J. Bower,[1] M. W. Bowers,[1] D. Boyle,[1] D. K. Bradley,[1] J. Bragg,[1] J. Braucht,[1] D. Brinkerhoff,[1] D. Browning,[1] S. Burkhart,[1] S. Burns,[1] B. Burr,[1] L. Burrows,[1] B. Butlin,[1] R. Cahayag,[1] D. A. Callahan,[1] P. Cardinale,[1] J. Carlson,[1] A. Casey,[1] C. Castro,[1] J. R. Celeste,[1] J. Celeste,[1] A. Chakicherla,[1] F. Chambers,[1] C. Chan,[1] C. Chang,[1] R. Chapman,[1] K. Charon,[1] Y. Chen,[1] T. Clancy,[1] B. Cline,[1] L. Clowdus,[1] D. Cocherell,[1] F. E. Coffield,[1] S. Cohen,[1] R. Costa,[1] A. J. Cox,[1] G. Curnow,[1] M. Dailey,[1] P. Danforth,[1] S. Dangi,[1] R. Darbee,[1] P. Datte,[1] J. Davis,[1] G. Deis,[1] E. L. Dewald,[1] P. DiNicola,[1] J. M. DiNicola,[1] S. Dixit,[1] J. Driscoll,[1] J. Dugorepec,[1] J. Duncan,[1] P. Dupuy,[1] E. Dzenitis,[1] M. Eckart,[1] S. L. Edson,[1] G. Edwards,[1] M. J. Edwards,[1] P. Edwards,[1] J. C. Ellefson,[1] C. Ellerbee,[1] G. Erbert,[1] W. Fabyan,[1] R. Fallejo,[1] B. Felker,[1] J. Fink,[1] M. Finney,[1] L. Finnie,[1] M. Fischer,[1] J. W. Florio,[1] A. Forsman,[1] C. Foxworthy,[1] M. Franks,[1] T. Frazier,[1] G. Frieder,[1] G. Frieders,[1] T. Fung,[1] C. Gibson,[1] E. Giraldez,[1] S. Glenn,[1] B. Golick,[1] H. Gonzales,[1] S. Gonzales,[1] M. Gonzalez,[1] J. Grippen,[1] S. M. Gross,[1] P. H. Gschweng,[1] G. Gururangan,[1] S. W. Haan,[1] S. Hahn,[1] B. J. Haid,,[1] J. Hamblen,[1] A. V. Hamza,[1] D. Hardy,[1] D. Hart,[1] R. Hartley,[1] C. A. Haynam,[1] G. M. Heestand,[1] M. Hermann,[1] G. Hermes,[1] D. Hey,[1] R. Hibbard,[1] D. E. Hinkel,[1] D. Hipple,[1] J. Hitchcock,[1] D. Hodtwalker,[1] J. P. Holder,[1] J. Hollis,[1] G. Holtmeier,[1] S. Huber,[1] A. Huey,[1] D. Hulsey,[1] S. Hunter,[1] T. Huppler,[1] M. Hutton,[1] N. Izumi,[1] J. Jackson,[1] M. Jackson,[1] K. S. Jancaitis,[1] D. Jedlovec,[1] T. Johnson,[1] B. Johnson,[1] M. Johnston,[1] O. S. Jones,[1] D. H. Kalantar,[1] J. Kamperschroer,[1] R. Kauffman,[1] G. Keating,[1] S. Kenitzer,[1] J. R. Kimbrough,[1] K. King,[1] R. K. Kirkwood,[1] K. Knittel,[1] T. Kohut,[1] K. Koka,[1] S. Kramer,[1] J. Krammen,[1] K. Krauter,[1] E. Krieger,[1] J. Kroll,[1] K. La Fortune,[1] V. Lakamsani,[1] O. L. Landen,[1] S. W. Lane,[1] J. Laney,[1] B. Langdon,[1] S. Langer,[1] N. Lao,[1] D. Larson,[1] D. LaTray,[1] S. Le Pape,[1] B. Lechleiter,[1] Y. Lee,[1] T. Lee,[1] J. Li,[1] J. Liebman,[1] J. D. Lindl,[1] S. F. Locke,[1] H. Loey,[1] R. London,[1] F. J. Lopez,[1] D. M. Lord,[1] R. Lowe-Webb,[1] J. Lown,[1] N. Lum,[1] R. Lyons,[1] T. Ma,[1] A. J. MacKinnon,[1] M. Magat,[1] T. N. Malsbury,[1] G. Markham,[1] D. Marquez,[1] R. Marquez,[1] A. Marsh,[1] S. Marshall,[1] I. Maslennikov,[1] J. Mauger,[1] M. Mauldin,[1] J. Mauvais,[1] J. McBride,[1] T. McCarville,[1] J. B. McCloud,[1] A. McGrew,[1] B. Mchale,[1] A. McPhee,[1] J. Meeker,[1] J. Merill,[1] E. Mertens,[1] P. Michel,[1] T. Mills,[1] R. Miramontes,[1] R. C. Montesanti,[1] M. Montoya,[1] J. Moody,[1] J. D. Moody,[1] K. Moreno,[1] J. Morris,[1] K. Morriston,[1] J. Nelson,[1] M. Neto,[1] J. Neumann,[1] E. Ng,[1] Q. Ngo,[1] B. Olejniczak,[1] R. E. Olson,[1] N. Orsi,[1] M. Owens,[1] E. Padilla,[1] T. Pannell,[1] T. Parham,[1] R. W. Patterson Jr.,[1] D. Pendlton,[1] F. Penko,[1] B. Pepmeier,[1] D. Petersen,[1] T. Phillips,[1] D. Pigg,[1] K. W. Piston,[1] K. Pletcher,[1] P. Rahul,[1] B. Raimondi,[1] J. E. Ralph,[1] R. Rampke,[1] B. Reid,[1] V. V. Rekow,[1] J. L. Reynolds,[1] J. Rhodes,[1] M. J. Richardson,[1] R. Rinnert,[1] B. Riordan,[1] A. Rivenes,[1] A. Rivera,[1] C. Roberts,[1] D. Roberts,[1] J. Robinson,[1] R. B. Robinson,[1] S. Robison,[1] O. Rodriguez,[1] S. Rogers,[1] M. D. Rosen,[1] G. Ross,[1] M. Runkel,[1] T. Runtal,[1] R. Sacks,[1] S. Sailors,[1] T. Salmon,[1] J. D. Salmonson,[1] R. Saunders,[1] J. Schaffer,[1] M. Schmitt,[1] M. B. Schneider,[1] K. S. Segraves,[1] M. Shaw,[1] M. Sheldrick,[1] R. Shelton,[1] M. Shiflett,[1] S. J. Shiromizu,[1] M. Shor,[1] L. Silv,[1] K. M. Skulina,[1] D. Smauley,[1] L. Smith,[1] B. Smith,[1] A. Solomon,[1] S. Sommer,[1] J. Soto,[1] N. Spafford,[1] P. T. Springer,[1] M. Stadermann,[1] F. Stanley,[1] T. Stone,[1] P. Stratton,[1] R. Strausser,[1] L. J. Suter,[1] W. Sweet,[1] M. F. Swisher,[1] J. Tappero,[1] J. Tassano,[1] J. S. Taylor,[1] C. A. Thomas,[1] A. Thomas,[1] A. Throop,[1] G. Tietbohl,[1] J. Tillman,[1] R. P. Town,[1] K. Tribbey,[1] D. Trummer,[1] J. Truong,[1] J. Vaher,[1] M. Valadez,[1] A. Van Prooyen,[1] G. Vergel de Dios,[1] M. Vergino,[1] S. Vernon,[1] J. Vickers,[1] G. Villanueva,[1] M. Vitalich,[1] L. Vo,[1] S. Vonfof,[1] F. Wade,[1] R. J. Wallace,[1] C. Warren,[1] A. Warrick,[1] J. Watkins,[1] S. Weaver,[1] P. Wegner,[1] M. Weingart,[1] J. Wen,[1] P. Whitman,[1] C. C. Widmayer,[1] H. Wilkens,[1] W. Williams,[1] E. A. Williams,[1] L. Willis,[1] M. Witte,[1] K. Work,[1] P. S. Yang,[1] B. K. Young,[1] K. P. Youngblood,[1] R. A. Zacharias,[1] T. Zaleski,[1] P. Zapata,[1] J. L. Kline,[2] G. A. Kyrala,[2] C. Niemann,[3] J. D. Kilkenny,[4] A. Nikroo,[4] B. Van Wonterghem,[5] L. J. Atherton,[5] and E. I. Moses[5]

[1] *Lawrence Livermore National Laboratory, Livermore, CA 94550, USA*
[2] *Los Alamos National Laboratory, Los Alamos, NM 87545, USA*
[3] *Department of Physics and Astronomy, University of California, Los Angeles, CA 90095, USA*
[4] *General Atomics, San Diego, CA , USA*
[5] *Lawrence Livermore National Laboratory, Livermore, CA 94551, USA*

We demonstrate the hohlraum radiation temperature and symmetry required for ignition-scale inertial confinement fusion capsule implosions. Cryogenic gas-filled hohlraums with 2.2 mm diameter capsules are heated with unprecedented laser energies of up to 1 MJ delivered by 192 ultraviolet laser beams on the National Ignition Facility. Optical laser backscatter measurements show that these hohlraums absorb 90 % of the incident laser power resulting in radiation temperatures of $T_{RAD} = 284$ eV and a symmetric implosion to a 100μm diameter hot core.

PACS numbers: 52.38.-r, 52.38.Hb, 52.38.Dx

The 192 laser beams of the National Ignition Facility (NIF) [1] have recently been commissioned [2] to deliver the laser energy and power required for heating ignition-scale hohlraums to indirect-drive inertial confinement fusion conditions. Efficient coupling of the laser beams and efficient heating of the hohlraum to radiation temperatures of 270 eV $\leq T_{RAD} \leq$ 300 eV are design goals for compressing the fusion capsule in the center of the hohlraum in a rocket-like spherical implosion. Ignition and significant fusion yield require centimeter-scale hohlraums that hold a 2.2 mm-diameter fusion capsule with approximately 0.2 mg of nuclear fuel. The fuel is prepared cryogenically into a solid deuterium-tritium ice layer surrounded by light ablator material [3]. The hohlraum radiation field heats the ablator compressing the fuel by x-ray ablation pressure to densities of 1000-times solid with a central hot spot that approaches temperatures of 10 keV from which the nuclear burn process is initiated [4–6].

Burning approximately 1/3 of the DT-fuel will result into 6.5×10^{18} fusion neutrons primarily from the $D + T =^4 He(3.5\text{ MeV}) + n(14.1\text{ MeV})$ process with a total yield of 15 MJ. The formation of the central hot spot and the assembly of the thermonuclear fuel requires implosions velocities of 350 km/s and a symmetrically compressed capsule to a sphere with a diameter of 60 μm. While round implosions have been demonstrated by controlling the laser beam power on the hohlraum wall either by directly tuning the power of individual beams [7–9] or more efficiently with self-generated plasma optics gratings on the NIF [10, 11], the implosion velocity and compression are directly related to the hohlraum radiation temperature and consequently to the absorbed laser energy in the hohlraum [12, 13].

In this letter, we present experiments of laser-heated ignition-size hohlraums with laser energies of up to 1 MJ that show 90 % coupling. Losses are due to Stimulated Raman Scattering (SRS) from the laser beams closest to the hohlraum axis that interact with the dense capsule blow-off plasma. At the mega-joule level we compensate for the *local* losses and demonstrate a symmetric implosion by properly choosing the laser wavelength of the heater beams. A shift of 0.28 nm between the inner and outer cones of beams provides symmetric x-ray drive by controlling the power distribution on the hohlraum wall. In addition, the experiments indicate a hot electron preheat of 250 J for electron energies above 170 keV, i.e., 0.03 % of total energy, and 14 % gold M-band radiation fraction for x-ray energies $E > 2$ keV. The latter is absorbed by a graded Ge dopant layer in the capsule tailoring the density profile at the ablator-ice interface and avoiding preheat of the ice fuel layer. The experimental hohlraum radiation temperatures scale with laser energy and hohlraum size according to the Marshak scaling [14] and are successfully modeled by radiation-hydrodynamic simulations using the code LASNEX [15]. The experimental data and modeling scale to a radiation drive of 300 eV for 1.1 – 1.2 MJ of absorbed laser energy.

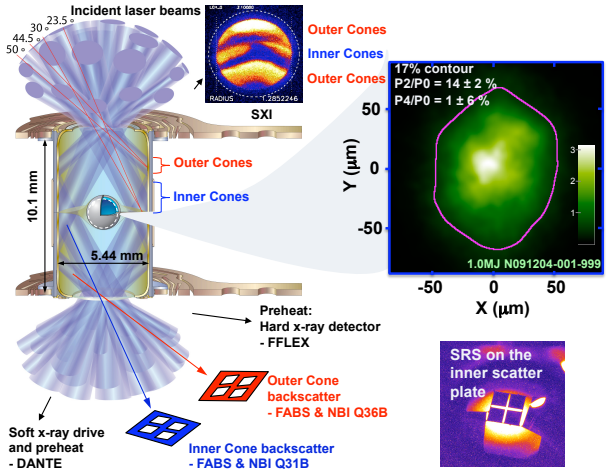

FIG. 1. Schematic of a hohlraum heated by 192 laser beams is shown along with various optical and x-ray diagnostics. The gated x-ray image from an implosion driven with 1 MJ laser energy shows symmetric 9 keV capsule x-ray emission at peak emission time, t = 20.9 ns. The hohlraum radiation temperature is measured through the LEH with the Dante detector while laser energy and power backscattered from the target is measured with temporally and spectrally resolved backscatter diagnostics using Full Aperture Back Scatter (FABS) and Near Backscatter Imager (NBI) detectors on two quads of beams on the 30° and 50° cones.

The experiments use cryogenic gas-filled gold hohlraums at temperatures of 20 K containing plastic capsules nominally filled to high densities of 8.2 mg cm^{-3} helium. Some capsules also contained traces of deuterium of up to 13 % atom fraction. The hohlraums are 1 cm long with a diameter of 5.44 mm and filled with helium or helium:hydrogen gas at densities of 0.65 – 1.3 mg cm^{-3}. In addition, experiments with reduced-scale hohlraums (84 %) have been performed

with length of 8.4 mm, diameter of 4.6 mm, and capsule diameters of $1.85 - 1.95$ mm. The hohlraums are heated with up to 192 laser beams through two laser entrance holes (LEHs) of 2.6 mm or 3.1 mm diameter on either end (Fig. (1)). The beams are arranged in four cones of beams; the inner cones of beams are at angles of 23.5° and 30° and the outer cones of beams are at 44.5° and 50° to the vertical axis.

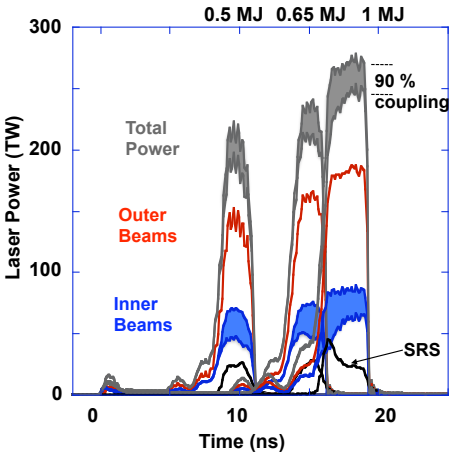

FIG. 2. The measured laser powers on the inner and outer cones of beams together with the total powers are shown along with the scattering losses by SRS. Cryogenic hohlraum experiments show (90^{+5}_{-3}) % absorbed laser energy.

Figure (2) shows the frequency-tripled laser power at a wavelength of 351 nm on the inner and outer cones of beams along with the total power. Reduced-scale hohlraum experiments (84 % of ignition scale) heated with 11 ns and 16 ns long heater beam pulses indicate 91% and 92 % coupling, respectively. For this scale, the coupling is found $2 - 3$ % lower than previously quoted [10, 16] due to improved analysis that include estimates of SRS on the 23.5° cone of beams. All hohlraum experiments, including ignition-scale hohlraums heated with up to 1 MJ, show 90 % absorbed laser energy or higher consistent with previous estimates [10].

Laser backscattering primarily occurs on the inner cones of beams while backscatter on the outer cones of beams is negligible. The total SRS losses are indicated as shaded areas in Fig. (2). We infer these losses from the absolute $30 - 100$ keV bremsstrahlung emission measurements with the Filter Fluorescer X-ray (FFLEX) detector. The spectrum can be fit with a two-temperature distribution [17] indicating a hot electron population with a temperature of $16.5 - 19$ keV produced by damping of the SRS-driven electron plasma (Langmuir) waves along with a high-temperature component at 50 keV. For the mega-joule heated hohlraum integrating the former and using the Manley-Rowe relations yields a total SRS loss of 100 kJ (±15 %) while integrating the latter [18, 19] results in hot electron preheat of 250 J (±50 %). Combining these findings with the SRS backscatter measurement of 45 kJ using FABS and NBI detectors on the 30° cone indicates a 55 kJ SRS loss on the 23.5° cone of beams.

Maintaining 90 % coupling for hohlraums driven by more than 0.5 MJ energy has been the result of optimizing the hohlraum gas fill species, density, and the polarization smoothing [20] choice. We replaced a 20 % helium, 80 % hydrogen mixture by atomic fraction with a pure He hohlraum gas fill. In addition, the polarization rotators on the inner cones of beams have been optimized. On NIF, a quad of four f-20 beams enter the target chamber through one effective f-8 optics assembly and overlay on target with two beams being equipped with polarization rotators; these have been arranged into a checkerboard geometry to optimize the overlap of beams with orthogonal polarization inside the hohlraum. These improvements have reduced SRS losses by a factor of 2 at 0.5 MJ and result in over 90 % coupling at 0.65 MJ. In going to the mega-joule level, we further increased the hohlraum size and reduced the fill pressure from 1.3 mg cm^{-3} to 0.94 mg cm^{-3}.

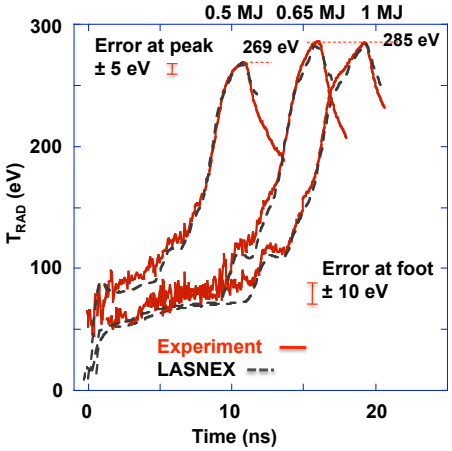

FIG. 3. Experimental and calculated hohlraum radiation temperatures are shown as function of time. Experiments with 11 ns and 16 ns long heater beam pulses use a reduced scale hohlraum (84 %), and data with the 19 ns long pulse are from the ignition-size hohlraum heated with 1 MJ laser energy.

Figure (3) shows experimental and calculated hohlraum radiation temperatures as function of time. These experiments reach peak drives of 269 eV to 285 eV, and both temporal dependence and peak values are in excellent agreement with radiation-hydrodynamic modeling using the code LASNEX. The data are inferred from measurements of the x-ray power, P, in the energy range of $0 < E_{X-ray} < 20$ keV out of the laser entrance hole (LEH) with the absolutely calibrated broadband x-ray spectrometer Dante [21].

From the measured radiant intensity the temperature can be inferred via $dP/d\Omega = A_{LEH}(t)\phi(t)\cos\theta\sigma T^4_{RAD}/\pi$. Here, θ is the view

angle of Dante towards the hohlraum axis. The dynamically varying source area, $A_{LEH}(t)$ is estimated from the $3-5$ keV x-ray images [22] of the LEH measured with the Static X-ray Imager, SXI, c.f. Fig. (1). The latter shows a reduction of the LEH diameter to 83 % of the initial value. Finally, the view factor ϕ relates the Dante measured drive with the radiation temperature seen by the capsule; this factor results in a $10-15$ eV corrections for these experiments.

The internal hohlraum radiation temperatures are modeled by balancing the absorbed laser power with the x-ray power radiated into the wall, P_W, absorbed by the capsule, P_{CAP}, and the power that escapes though the LEH, P_{LEH},

$$\begin{aligned} &\eta_{\rm CE}\,(P_{\rm L}-P_{\rm Backscatter}) \qquad (1)\\ &= P_{\rm W}+P_{\rm LEH}+P_{\rm CAP}\\ &= \sigma T_{\rm RAD}^4\,[(1-\alpha_{\rm W})A_{\rm W}+A_{\rm LEH}+(1-\alpha_{\rm CAP})A_{\rm CAP}] \quad . \end{aligned}$$

With $\eta_{\rm ce}$ being the x-ray conversion efficiency from laser power to soft x-rays [23] and σ is the Stefan-Boltzmann constant; $\alpha_{\rm W}$ and $\alpha_{\rm CAP}$ are the x-ray albedo of the hohlraum wall and the capsule, respectively. The albedo is defined as the ratio of re-emitted over incident x-rays. The hohlraum wall area, laser entrance hole area, and capsule surface area are denoted by $A_{\rm W}$, $A_{\rm LEH}$ and $A_{\rm CAP}$, respectively. Equation (1) yields the observed scaling of peak temperature when increasing the absorbed power at 84 % hohlraum scale. Further, including the fact that hohlraum wall loss scales as $P/A_{\rm W}\times t^{0.6}$, Eq. (1) reproduces the observed constant $T_{\rm RAD}$ for the increased hohlraum wall area and pulse duration.

Figure (4) show the experimental peak radiation temperatures for various hohlraum experiments as function of the absorbed energy along with results from radiation hydrodynamic modeling with the code LASNEX that use the detailed configuration accounting model for x-ray opacities [25]. Generally, we ovbserve good agreement between data and modeling; in particular, at ignition scale the data extrapolate to a hohlraum drive approaching 300 eV at $1.1-1.2$ MJ absorbed energy. Also shown in Fig. (4) are the Marshak scaling results [14] of Eq. (1) assuming a conversion efficiency of $\eta_{ce}=0.9$ and the albedo calculated according to [24]. The latter increases according to the data and integrated modeling and provides a good match to the experimental data at both hohlraum scales

In summary we have demonstrated efficient heating of ignition-scale hohlraums with radiation temperature and illumination symmetry required for inertial confinement fusion capsule implosions. The hohlraums show 90 % coupling of the incident laser energy and scale with radiation temperature according to radiation hydrodynamic calculations and modeling. Future studies will explore further improvements in hohlraum drive including experiments with optimized wall areas and hohlraum fill densities as well as hohlraums with higher-Z wall materials and higher wall opacities [26–28], e.g., uranium.

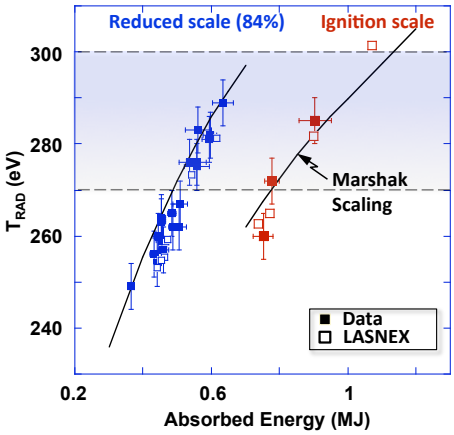

FIG. 4. Experimental and calculated hohlraum radiation temperatures are shown as function of the absorbed laser energy into the hohlraum. The measured values are from the broadband x-ray spectrometer Dante and radiation hydrodynamic modeling use the code LASNEX with detailed configuration accounting. The Marshak scaling equates the absorbed laser power with a x-ray conversion efficiency of 90 % with radiation losses according to Eq. (1). The results indicate that ≥ 1.1 MJ of absorbed laser energy will be required to drive an ignition hohlraum to radiation temperatures of $T_{RAD}=300$ eV.

Acknowledgements

This work performed under the auspices of the U.S. Department of Energy by Lawrence Livermore National Laboratory under Contract DE-AC52-07NA27344.

[1] E. Moses, C. R. Wuest, Fusion Sci. Tech. **47**, 314 (2005).
[2] C. Haynam *et al.*, Appl. Optics **46** 3276 (2007).
[3] S.W. Haan *et al.*, Phys. Plasmas, **2**, 2480 (1995).
[4] J.D. Lindl, Phys. Plasmas **2**, 3933 (1995).
[5] J.D. Lindl *et al.*, Phys. Plasmas, **11** (2), 339 (2004).
[6] S. Atzeni, J. Meyer-ter-Vehn, The Physics of Inertial Fusion (Oxford Univ. Press, New York, 2004).
[7] A. A. Hauer *et al.*, Phys. Plasmas **2**, 2488 (1995).
[8] O. L. Landen *et al.*, Phys. Plasmas **6**, 2488 (1999).
[9] R. E. Turner *et al.*, Phys. Plasmas **7**, 333 (2000).
[10] S. H. Glenzer *et al.*, Science **327**, 1228 (2010).
[11] P. Michel *et al.*, Phys. Plasmas **17**, 056305 (2010).
[12] L. J. Suter *et al.*, Phys. Rev. Lett. **73**, 2328 (1994).
[13] W. J. Krauser, Phys. Plasmas **3**, 2084 (1996).
[14] R. E. Marshak, Phys. Fluids **1**, 24 (1958).
[15] G. B. Zimmerman and W. L. Kruer, Comments Plasma Phys. Control. Fusion **2**, 85 (1975).
[16] N. Meezan *et al.*, Phys. Plasmas **17**, 056304 (2010).
[17] C. Thomas, Phys. Rev. E **81**, 036413 (2010).
[18] K. A. Brueckner, Phys. Rev. Lett. **37**, 1247 (1976).

[19] R. P. Drake *et al.*, Phys. Rev. A **40**, 3219 (1989).
[20] E. Lefebvre *et al.*, Phys. Plasmas **5**, 2701 (1998).
[21] E. L. Dewald *et al.*, Rev. Sci. Instrum. **75**, 3759 (2004).
[22] M. B. Schneider *et al.*, Rev. Sci. Instrum. **100** (2010).
[23] E. Dattolo, *et al.*, Phys. Plasmas **8**, 260 (2001).
[24] R. Sigel *et al.*, Phys. Rev. Lett. **65**, 587 (1990).
[25] J. L. Kline *et al.*, Phys. Rev. Lett. *submitted* (2010).
[26] R. E. Olson *et al.*, Rev. Sci. Instrum. **74**, 2186 (2003).
[27] J. Schein *et al.*, Phys. Rev. Lett. **98**, 175003 (2007).
[28] O. S. Jones *et al.*, Phys. Plasmas **14**, 056311 (2007).